PROCEEDINGS of the
23rd International Congress on Acoustics
9 to 13 September 2019 in Aachen, Germany

Calculation of the fan rotational speed based on flyover recordings for improving aircraft noise prediction models

Roberto MERINO–MARTINEZ[(1)]; Mirjam SNELLEN[(1)]; Dick G. SIMONS[(3)]

[(1)]Delft University of Technology, the Netherlands, r.merinomartinez@tudelft.nl

Abstract

The enforcement of noise control regulations around airports usually depends on the estimations of aircraft noise prediction models. Current best–practice noise contour calculation methods assume default engine thrust values depending on the engine type and the altitude of the aircraft. These prediction tools provide a single noise level for a certain aircraft type in a certain flight phase and at a specific distance from the observer. In practice, however, changes in the thrust occur and cause variations in the noise levels of several decibels. In this paper, an approach is presented to estimate the fan rotational speed N1% (and hence the thrust) directly from flyover audio recordings. This method estimates the blade passing frequency (BPF) of the fan by searching its characteristic tonal peak (and its higher harmonics) and accounting for the Doppler effect. This method was applied to more than 400 measurements of Airbus A330–300 aircraft. The results show a significant correlation between the recorded noise levels and the fan rotational speed, explaining up to 43% of the variability in noise levels. Considering the calculated N1% values in the noise prediction models notably increases the agreement of the estimations with the recorded noise levels.

Keywords: Aircraft noise, Turbofan noise, Noise prediction models

1 INTRODUCTION

Due to the increasingly importance of aircraft noise because of the continuous growth in air traffic, obtaining precise information about the aircraft noise levels is essential for properly enforcing environmental laws around airports, route management and and land–use planning [1, 2].

The typical approach for estimating aircraft noise levels is based on legal compliance methods, such as those described in Document 29 of the ECAC (European Civil Aviation Conference) [3], which allow for the calculation of noise contours around airports to estimate the average noise exposure of aircraft operations over a relatively long period of time and set noise limits. This type of methodology can be called *best practice* since relatively large assumptions are made, either for practical reasons or due to the lack of detailed data. The noise levels are estimated for each operation using *look–up* tables, such as the noise–power–distance (NPD) tables, whereby the aircraft's thrust settings and the distance to the observer are the main inputs. Previous comparisons between aircraft noise prediction models and experimental measurements [4–7] showed that differences of several decibels exist between modeled and measured noise levels, which can lead to important errors when assessing the annoyance experienced by the population living around airports. For example, a mere difference of 1 dB in the predictions can lead to changes of about 20% in the noise contours [8]. Therefore, experimental validations and potential improvements of these models are of great interest [2].

Other more sophisticated, semi–empirical aircraft noise prediction methods, such as ANOPP [9] or PANAM [10] model the sound emission and propagation separately and provide more accurate predictions, but they require very detailed input data, which are not typically publicly available [5]. In addition, these programs are normally not accessible to other users and are limited to a small number of aircraft types. Therefore, this paper focuses on the *best practice* method of ECAC's Doc. 29. For a more detailed explanation on how to use this method, the reader is referred to [2, 3].

These simpler *best practice* prediction tools, such as the NPD tables, provide a single noise level for a certain aircraft type, in a certain flight phase and at a specific distance from the observer [11, 12]. Previous studies

[13–15], however, showed that changes in certain aircraft settings (especially the fan rotational speed) produce variations in the noise levels of several decibels. Not accounting for this fact can considerably hamper an accurate calculation of noise contours. The noise prediction models use relatively simple estimations (the so–called thrust profile) for the net engine thrust for each flight phase.

In order to evaluate the current assumptions regarding net thrust made by the noise contour models, the actual engine fan settings $N1\%$ (i.e., the relative fan rotational speed) and the distance between the aircraft and the observer need to be determined. The term *engine fan setting* [4, 13–15] refers to the ratio between the fan rotational speed (in rpm), n, and the maximum fan rotational speed, $n_{\max}$, i.e., $N1\% = 100\,n/n_{\max}$ because it refers to the low–pressure shaft of the engine, on which the fan is mounted. Even though the actual aircraft settings are recorded by airlines, these data are not publicly disclosed for reasons such as pilot privacy and to ensure the operation business strategies of airlines. To compensate for this lack of information, a method to determine $N1\%$ based solely on audio files is proposed and described in this paper. Whereas some of the aforementioned studies [4, 7, 13–18] made use of phased microphone arrays to analyze the noise contributions of different aircraft components, the present research only studies the total aircraft noise levels recorded by an individual microphone from the Noise Monitoring System (NOMOS) around Amsterdam Airport Schiphol in the Netherlands [2].

Thus, the aim of this paper is to investigate the effects of considering the instantaneous thrust setting on the noise level predictions, rather than employing tabulated values as in practice. A large set of experimental data, containing more than 400 flyovers of Airbus A330–300 (henceforth Airbus 333) aircraft under different operational modes (arrivals and departures), was considered to compare the $N1\%$ values used by the models with those found experimentally. A correlation analysis was performed between the recorded noise levels and the measured engine fan settings to assess the importance of this parameter in the noise emissions. Lastly, a comparison between the noise levels predicted using the NPD tables and those recorded experimentally is also presented.

2 EXPERIMENTAL SETUP

The study is based on 433 audio files recorded by one noise monitoring terminal (NMT 14) in the surroundings of Amsterdam Airport Schiphol in 2016. The flyovers correspond to approaches (221) and departures (212) of Airbus 333 aircraft, which is a wide–body, twin–engine jet airliner designed for medium– to long–range operations. Almost all the aircraft considered were equipped with engines from the CF6–80E1A family, which are the ones considered for this study. The extension to more aircraft types and measurement locations can be found in [2].

The NOMOS system continuously measures the noise in residential areas around Amsterdam Airport Schiphol using calibrated Brüel & Kjær microphones. The microphones start recording whenever a certain threshold sound pressure level (L_{p}) is exceeded. The measurement point is located at Hoofdweg 1730, Abbenes in the Netherlands (latitude 52.2353764 °, longitude 4.5937646 ° and altitude -3 m).

Unfortunately, to reduce data storage, the NOMOS audio files are filtered and resampled with a sampling frequency of 8 kHz when stored, which causes a loss of all the spectral information for frequencies higher than 3500 Hz [2]. Hence, the noise metrics recorded by NOMOS (before the data compression) were used as a reference. The maximum Overall A–weighted Sound Pressure Level ($L_{\mathrm{p,A,max}}$) was employed in this study but the same conclusions apply to other metrics such as the sound exposure level (SEL or $L_{\mathrm{p,A,e}}$) or the effective perceived noise level (EPNL) [2].

The trajectories of the aircraft flyovers were determined using ground radar data from air traffic control, which is recorded every 4 seconds and interpolated linearly in between [2]. The average minimum distance to the observer ($\bar{r}_{\min}$) for approaches (640 m) was considerably shorter than for departures (1110 m). The variability in the minimum distances $r_{\min}$ is also considerably smaller for approaches (70 m) than for departures (about 730 m) because all aircraft follow the instrument landing system approach. In order to have a more fair comparison in the noise levels, these differences in distances to the observer were partially accounted for using a simple

correction factor ΔL_p (considering approaches and departures separately) for the sound spreading which was added to the recorded $L_{p,A,max}$ values

$$\Delta L_p = 20 \log \left(\frac{r_{min}}{\bar{r}_{min}} \right). \tag{1}$$

This correction factor is positive for minimum distances to the observer larger than the average ($r_{min} > \bar{r}_{min}$) and vice versa, i.e., the noise levels of aircraft flying further away than $\bar{r}_{min}$ are increased and vice versa.

The weather conditions showed similar values along the duration of the measurements. The temperatures were used to calculate the sound speed and certain parameters required for the net thrust estimations performed by the NPD tables, and the wind velocities for calculating the true airspeeds of the aircraft together with the ground radar data [2]. The velocities presented similar values (about 70 m/s) for both approaches and departures at the moment when the distance was minimum to the observer. The recorded flyovers had a variability in velocity for both operation types of about 20 m/s.

3 ESTIMATION OF AIRCRAFT ENGINE SETTINGS

The rotation of the turbofan produces tonal sound because of the interaction between the fan blades and the stator vanes. The fundamental frequency of this sound, f_1, is called blade passing frequency (BPF) and depends on the fan rotational speed n:

$$\text{BPF} = f_1 = \frac{Bn}{60}, \tag{2}$$

where B is the number of fan blades (38 in this case).

Higher harmonics of the BPF are usually found as well in the sound signature of aircraft flyovers. The frequencies of these harmonics, f_k, are multiples of the BPF ($f_k = k f_1,\ k = 1, 2, 3 \ldots$). Unfortunately, due to the relatively low maximum frequency available in this study (3500 Hz), few higher harmonics (up to the fifth) were found in the spectrograms in practice.

The Doppler effect due to the relative motion of the aircraft with respect to the observer needs to be accounted for in the fan rotational speed estimation process. The expression for the Doppler–shift (f'/f) between the observed frequency f' and the emitted frequency f is

$$\frac{f}{f'} = \frac{1}{1 - \|\boldsymbol{M}\| \cos(\theta)}, \tag{3}$$

where $\|\cdot\|$ is the Euclidean norm of the vector, $\boldsymbol{M}$ is the Mach number vector, $\boldsymbol{M} = \boldsymbol{V}/c$, $\boldsymbol{V}$ is the source velocity vector, c is the speed of sound and θ is the angle between the position vector of the source with respect to the observer, $\boldsymbol{r}$, and $\boldsymbol{V}$.

The variation of the polar emission angle θ and the Doppler shift for an example flyover recording are presented in Fig. 1a. The Doppler effect can be observed in the varying frequency of the engine fan tones in the spectrograms depicted in Figs. 1b and 1c as black curves.

Thus, the first step in this analysis is to determine the BPF value for each flyover audio recording and then calculate the fan rotational speed n using Eq. (2). The inputs necessary for this method are the trajectory and engine characteristics of the aircraft and the audio recording of the flyover. The expected continuous and monotonically decreasing Doppler shift can be estimated using the aircraft trajectory and Eq. (3), see Fig. 1a. Afterwards, a least–squares curve–fitting process is performed to ensure that the measured narrow–band engine fan tones in the signal's spectrogram agree with the predicted Doppler shift, see thick black line in Fig. 1b. The spectrograms are calculated by using 2048 samples per time block with Hanning windowing and a 50% data overlap. For each time step, peaks over a certain threshold are considered as candidates for the BPF. Afterwards, the characteristic Doppler–shifted curves corresponding to the fan tonal noise are searched for by

using these peaks. First, the BPF is searched for in the spectrogram within a predefined frequency band over time, depending on the operation mode and engine characteristics. Changes in the engine fan settings performed by the pilot during the recording time or due to the turbulence in the atmosphere can also cause "bumps" in the curves representing the engine fan tones see Fig. 1c. These irregularities can be accounted for by allowing a small increase (or decrease) in the Doppler–shifted tone frequency with respect to time. The allowable increase or decrease is defined by the user. The presence of higher harmonics is also evaluated by searching for multiples of the estimated BPF and serves as a further confirmation that the obtained BPF value is correct, see Fig. 1c where four additional harmonics are clearly detected. This process provides a (Doppler–corrected) BPF value (for the instant when $r = r_{\min}$) and, therefore, an $N1\%$ value. The obtained $N1\%$ needs to be checked to confirm that it falls within the typical range depending on the aircraft operation (approach or departure). In case the provided $N1\%$ value is not realistic, the whole process is repeated using a different search frequency band for the BPF, i.e., a different initial value for the BPF.

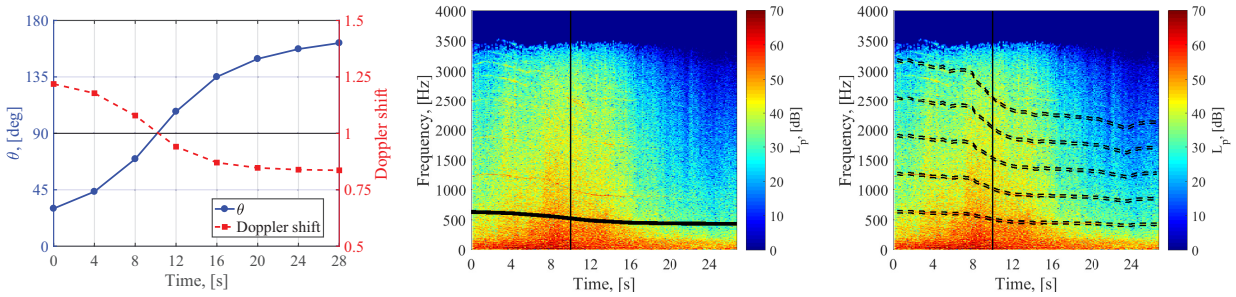

(a) (b) (c)

Figure 1. (a) Angle θ and Doppler shift during an example recording. Spectrograms of the audio signal with: (b) Curve fitted to the Doppler shift. (c) Detected engine tones. The vertical solid black line represents the time with $r = r_{\min}$.

4 RESULTS

4.1 Comparison between measured and modeled engine fan settings

Figure 2a shows that the fan rotational speeds are higher during departure ($N1 = 90\%$) than during approach ($N1 = 70\%$), as expected. However, larger variabilities are found in $N1\%$ during approach, with differences of about 30%, whereas during departure these differences are roughly 10%, which indicates that pilots need to adjust the throttle to keep the aircraft on the desired flight path during approach, but for departures the throttle is more fixed. The predicted $N1\%$ values using ECAC's Doc. 29 approach [2, 3] for these cases are plotted as black dots on the right of each box plot. For approach, this value falls within the 25^{th} and the 75^{th} percentiles (i.e., the box) of the experimental values, although below the median of these. For departures, on the other hand, the $N1\%$ value considerd by the NPD tables is slightly higher.

The box plot in Fig. 2b presents the variations in the $L_{\text{p,A,max}}$ metric provided by NOMOS and corrected for the distance following Eq. (1). The median values for both cases are comparable and between 65 and 70 dBA. However, it should be kept in mind that the distance correction of Eq. (1) is applied to each operation case individually, meaning that the higher value of $\bar{r}_{\min}$ for departures is not accounted for. That is why departures have comparable $L_{\text{p,A,max}}$ values as approaches. The predicted noise levels by the NPD tables for the selected flyovers are plotted as black lines on the right of the box plots, showing a satisfactory agreement for approaches but a considerable overestimation for departures. In general, variabilities in $L_{\text{p,A,max}}$ of about 20 dBA are observed in the experimental data for both cases, whereas the NPD results show a spread of only 3 dB for approach and 7 dB for departure.

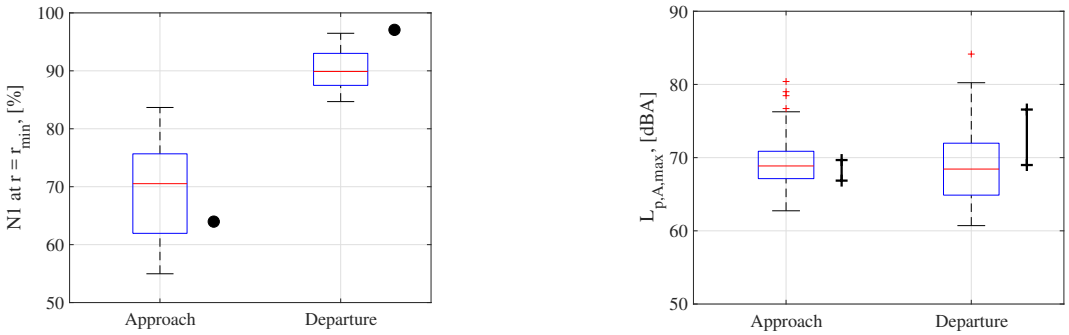

(a) (b)

Figure 2. Box plots indicating the variability of the: (a) Calculated $N1\%$ at $r = r_{\text{min}}$. (b) Measured $L_{\text{p,A,max}}$. The red crosses represent the outliers and the black dots and lines on the right of the boxes denote the estimations of the NPD tables.

4.2 Correlation analysis of noise level variations

The results of the correlation analysis between the recorded $L_{\text{p,A,max}}$ and the calculated engine fan settings ($N1\%$) at $r = r_{\text{min}}$ are presented in Figs. 3a and 4a. The correlation coefficient ρ, the coefficient of determination ρ^2 and the p–value are included in the legend of each graph. A common criterion to consider a correlation significant is that the p–value should be lower than 0.05 [15]. Following this criterion, the two correlations observed are deemed as significant. A coefficient of determination between $N1\%$ and $L_{\text{p,A,max}}$ of around 0.3 was found for the approaches. Similar values were obtained by Snellen *et. al.* [14] for landings of Boeing 737 and Fokker 70 aircraft. A higher value for ρ^2 (around 0.43) was found for the departure operations in Fig. 4a. This is expected because engine noise is supposed to be more dominant during departure than during approach [16], so a stronger correlation with the engine fan settings is justified.

No significant correlation was found between the recorded $L_{\text{p,A,max}}$ and the aircraft true airspeed at $r = r_{\text{min}}$ [2].

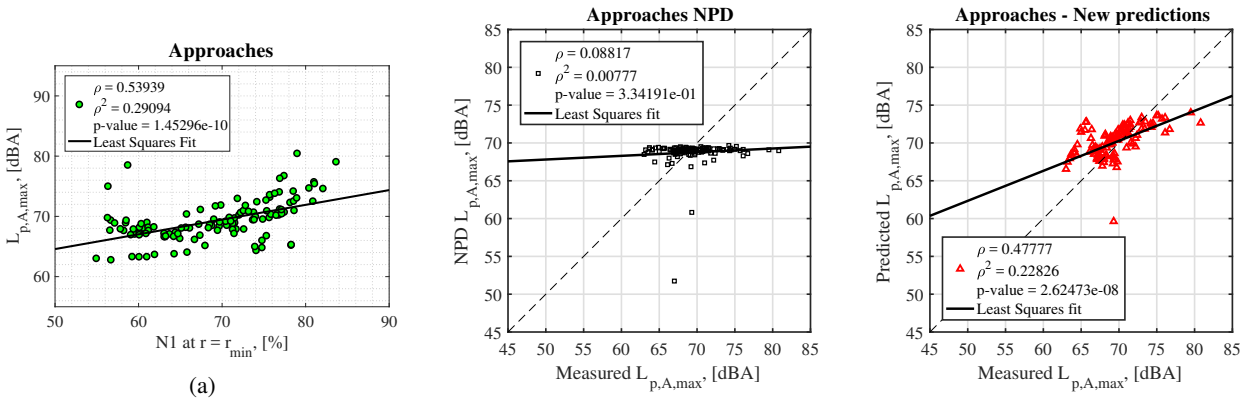

(a) (b) (c)

Figure 3. (a) Correlation analysis between $L_{\text{p,A,max}}$ and $N1\%$ at $r = r_{\text{min}}$ for approaches. Recorded $L_{\text{p,A,max}}$ vs. modeled $L_{\text{p,A,max}}$ using (b) default or (c) experimental $N1\%$ values for approaches.

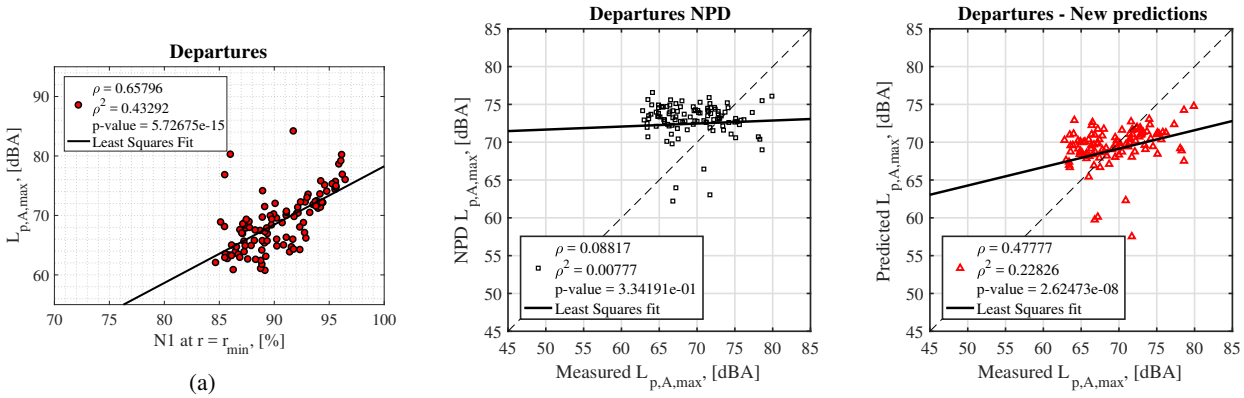

(a) (b) (c)

Figure 4. (a) Correlation analysis between $L_{\mathrm{p,A,max}}$ and $N1\%$ at $r = r_{\mathrm{min}}$ for departures. Recorded $L_{\mathrm{p,A,max}}$ vs. modeled $L_{\mathrm{p,A,max}}$ using (b) default or (c) experimental $N1\%$ values for departures.

Table 1. Average error (ε), average of the absolute values of the errors ($\varepsilon_{\mathrm{abs}}$), and standard deviation (σ) for $L_{\mathrm{p,A,max}}$ predictions with the NPD tables' default estimations of $N1\%$ (named as NPD) and using the $N1\%$ values obtained experimentally (named as Exp). All the values are in dBA.

Parameter	Approach	Departure
$\varepsilon_{\mathrm{NPD}}$	1.65	-2.97
$\varepsilon_{\mathrm{Exp}}$	-0.64	0.46
$\varepsilon_{\mathrm{NPD,\,abs}}$	2.65	5.38
$\varepsilon_{\mathrm{Exp,\,abs}}$	2.18	3.78
σ_{NPD}	3.58	6.05
σ_{Exp}	3.07	5.66

4.3 Comparison of recorded noise levels with modeled ones

In order to assess the importance of including the more accurate estimations of the $N1\%$ values obtained with the method introduced in this paper compared to the default ones used in the NPD tables, a comparison with the recorded NOMOS data was made twice: 1) considering the default $N1\%$ estimations by the NPD tables and 2) using the $N1\%$ values found experimentally. It should be noted that the distance correction of Eq. (1) was not applied in the $L_{\mathrm{p,A,max}}$ results shown in this section, since the NPD tables already account for the effects of the distance to the aircraft, r.

The results of both comparisons are gathered in Figs. 3 (b and c) and 4 (b and c) for approaches and departures, respectively. The diagonal black dashed line in Figs. 3 and 4 represents a perfect agreement between estimated and measured $L_{\mathrm{p,A,max}}$ levels ($\rho = 1$). The least squares fit for each case is also plotted. Considering the experimental $N1\%$ values produces a better agreement between the modeled and measured values of $L_{\mathrm{p,A,max}}$ and a five–fold increase of the correlation coefficient.

The average error (ε) and the average of the absolute values of the errors ($\varepsilon_{\mathrm{abs}}$) made by both predictions (using default or calculated $N1\%$ values) for each case are presented in Table 1. The error is defined as the difference between the measured and the estimated $L_{\mathrm{p,A,max}}$. Hence, $\varepsilon > 0$ means that the model underpredicts the actual noise levels and vice versa. The standard deviations of these errors, σ, are also included in Table 1. On average, including the experimental estimations of $N1\%$ reduces ε by 1 dBA and $\varepsilon_{\mathrm{abs}}$ and σ by 0.5 dBA each. Despite this improvement, there is still a significant discrepancy between the noise measurements and the noise model predictions. Additionally, it can be observed that in all the graphs there are several outliers that

are severely underpredicted by both NPD predictions by up to 15 dBA.

It should be noted that in this research, the experimental values of the aircraft velocity or altitude have been used for the NPD calculations, instead of using default tabulated ones, as usual. Therefore, the actual NPD estimations for $L_{\mathrm{p,A,max}}$ are most probably even less accurate than those presented here. Hence, the error reduction obtained by using more accurate input values could be even higher in reality. The approach of including the actual aircraft parameters was taken to isolate the influence of the choice of $N1\%$ for NPD predictions.

5 CONCLUSIONS

An automatic approach to determine the engine fan settings ($N1\%$) directly from flyover audio recordings was proposed in this paper, in order to consider more precise values of this parameter as input for prediction models, rather than tabulated default values. This method was employed on a large data set of more than 400 Airbus A330–300 aircraft flyovers recorded by the NOMOS system around Amsterdam Airport Schiphol.

A large variability was observed in the values of $N1\%$ obtained experimentally, compared to the default values assumed by the noise models. Significant correlations were found between the calculated $N1\%$ values and the measured noise levels. Introducing the $N1\%$ values obtained experimentally in the predictions reduced the errors made with respect to the noise level recordings. However, there is still a remaining error and a large variability in the noise levels unexplained by the noise prediction models.

After noticing the limitations of the noise prediction model employed in this paper, it is recommended to improve such models, especially by employing more accurate individual flight parameters or accounting for the strong influence of $N1\%$ in the noise levels. This recommendation is especially valid for more sophisticated purposes, such as noise abatement studies, rather than studies on the average exposure noise levels over long time periods, where errors in the model estimates can balance out.

Additional research with other aircraft types is encouraged, especially with recordings containing a larger frequency range (i.e., no undersampled as here). Moreover, repeating this study using other noise metrics, such as EPNL or new sound quality metrics [6, 19], is of high interest to better estimate the psychoacoustic annoyance around airports.

ACKNOWLEDGEMENTS

The authors would like to acknowledge the support received by Sander J. Heblij and Dick H. T. Bergmans throughout this project. They also want to thank Michael Arntzen from Amsterdam Airport Schiphol for providing the experimental data and critical thinking preparing this paper. The authors also acknowledge Henk Veerbeek from the Netherlands Aerospace Centre (NLR) for providing data about the engines.

REFERENCES

[1] Merino-Martinez R. Microphone arrays for imaging of aerospace noise sources. Delft University of Technology; 2018. ISBN: 978–94–028–1301–2.

[2] Merino-Martinez R, Heblij SJ, Bergmans DHT, Snellen M, Simons DG. Improving Aircraft Noise Predictions by Considering the Fan Rotational Speed. Journal of Aircraft. 2019;56(1):284–294.

[3] ECAC.CEAC Doc. 29. Report on Standard Method of Computing Noise Contours around Civil Airports. Volume 2: Technical Guide. Neuilly sur Seine Cedex, France: European Civil Aviation Conference (ECAC); 2016. 4th edition.

[4] Merino-Martinez R, Bertsch L, Snellen M, Simons DG. Analysis of landing gear noise during approach. In: 22nd AIAA/CEAS Aeroacoustics Conference. May 30 – June 1 2016. Lyon, France; 2016. AIAA paper 2016–2769.

[5] Zellmann C, Schäffer B, Wunderli JM, Isermann U, Paschereit CO. Aircraft Noise Emission Model Accounting for Aircraft Flight Parameters. Journal of Aircraft. 2017 March–April;55(2):682–695.

[6] Merino-Martinez R, Vieira A, Snellen M, Simons DG. Sound quality metrics applied to aircraft components under operational conditions using a microphone array. In: 25th AIAA/CEAS Aeroacoustics Conference. May 20 – 24 2019. Delft, The Netherlands; 2019. AIAA paper 2019–2513.

[7] Merino-Martinez R, Neri E, Snellen M, Kennedy J, Simons DG, Bennett GJ. Analysis of nose landing gear noise comparing numerical computations, prediction models and flyover and wind–tunnel measurements. In: 24th AIAA/CEAS Aeroacoustics Conference. June 25 – 29 2018. Atlanta, Georgia, USA; 2018. AIAA paper 2018–3299.

[8] Smith BS, Camargo HE, Burdisso RA, Devenport WJ. Development of a Novel Acoustic Wind Tunnel Concept. In: 11th AIAA/CEAS Aeroacoustics Conference. May 23 – 25 2005. Monterey, California, USA; 2005. AIAA paper 2005–3053.

[9] Kontos KB, Janardan BA, Gliebe PR. Improved NASA–ANOPP Noise Prediction Computer Code for Advanced Subsonic Propulsion Systems. Volume 1: ANOPP Evaluation and Fan Noise Model. NASA CR–195480; 1996. NASA CR–195480.

[10] Bertsch L, Dobrzynski W, Guérin S. Tool Development for Low–Noise Aircraft Design. Journal of Aircraft. 2010 March–April;47(2):694–699.

[11] Procedure for the Calculation of Airplane Noise in the Vicinity of Airports, Aerospace Information Report AIR 1845. 400 Commonwealth Drive, Warrendale, PA 15096: Society of Automotive Engineers, Inc. (SAE) - Committee on Aircraft Noise (SAE A-21); 1986. 1845.

[12] Recommended method for computing noise contours around airports (ICAO Circular 205–AN/1/25). Montreal, Canada.: International Civil Aviation Organization (ICAO); 1988. 9911.

[13] Snellen M, Merino-Martinez R, Simons DG. Assessment of aircraft noise sources variability using an acoustic camera. In: 5th CEAS Air & Space Conference. Challenges in European Aerospace. September 7 – 11 2015, Delft, Netherlands. Paper 2015–019. Council of European Aerospace Societies;. .

[14] Snellen M, Merino-Martinez R, Simons DG. Assessment of noise level variability on landing aircraft using a phased microphone array. Journal of Aircraft. 2017;54(6):2173–2183.

[15] Merino-Martinez R, Snellen M, Simons DG. Determination of Aircraft Noise Variability Using an Acoustic Camera. In: 23rd International Congress on Sound and Vibration, July 10 – 14 2016, Athens, Greece; 2016. .

[16] Merino-Martinez R, Snellen M, Simons DG. Functional beamforming applied to imaging of flyover noise on landing aircraft. Journal of Aircraft. 2016 November–December;53(6):1830–1843.

[17] Merino-Martinez R, Snellen M, Simons DG. Functional Beamforming Applied to Full Scale Landing Aircraft. In: 6th Berlin Beamforming Conference, February 29 – March 1 2016, Berlin, Germany. GFaI, e.V., Berlin; 2016. BeBeC–2016–D12.

[18] Merino-Martinez R, Neri E, Snellen M, Kennedy J, Simons DG, Bennett GJ. Comparing flyover noise measurements to full–scale nose landing gear wind–tunnel experiments for regional aircraft. In: 23rd AIAA/CEAS Aeroacoustics Conference. June 5 – 9 2017. Denver, Colorado, USA; 2017. AIAA paper 2017–3006.

[19] Merino-Martinez R, Pieren R, Snellen M, Simons DG. Assessment of the sound quality of wind turbine noise reduction measures. In: 26th International Congress on Sound and Vibration, July 7 – 11 2019, Montreal, Canada; 2019. .